Experimetal study of turbulence effect on underwater optical wireless communictions

Zahra Vali,[1] Asghar Gholami, [1,*] Zabih Ghassemlooy,[2] Masood Omoomi,[1] David G. Michelson[3]

[1] *Department of Electrical and Computer Engineering, Isfahan University of Technology, Isfahan 8415683111, Iran*
[2] *Optical Communications Research Group, Physical and Electrical Engineering Department, Northumbria University, Newcastle Upon Tyne, UK, NE1 8ST*
[3] *Department of Electrical and Computer Engineering, University of British Columbia, Vancouver, Canada, V6T1Z4*

**Corresponding author: gholami@cc.iut.ac.ir*

Received XX Month XXXX; revised XX Month, XXXX; accepted XX Month XXXX; posted XX Month XXXX (Doc. ID XXXXX); published XX Month XXXX

Underwater optical wireless communications (UOWC) performance is affected by turbulence. However, not much research has been carried out to estimate the probability density function (PDF) of the received optical power. In this paper, we investigate the turbulence effect on UOWC using a new experimental setup with a variable link span in a water pool. Different turbulence levels are created by changing the temperature and the rate of an injected water flow in the pool in order to obtain the PDF. Results show that lognormal distribution fits well with the measured PDF up to the scintillation index value of 0.07. In UOWC systems the link span is one of the main factor influencing fluctuations of the received optical power, which has not been investigated. In this work, we obtain the scintillation index and turbulence induced power loss for a range of turbulence strengths and for a transmission link span of up to 12 m. Finally, we show that there is a good agreement between the experimental and simulated results.

OCIS codes: *(060.4510) Optical communications; (010.4455) Oceanic propagation; (010.7060) Turbulence; (290.5930) Scintillation.*

http://dx.doi.org/10.1364/AO.99.099999

1. INTRODUCTION

Underwater optical wireless communications (UOWC) is an emerging technology, which can provide high-speed communications within the blue-green wavelength band. However, there are a number of environmental factors, which limit the performance of UOWC links. Most of the experimental investigations reported on UOWC have focused on the effect of absorption and multiple scattering on the propagating optical beam [1-5]. In addition, in recent years we have seen experimental investigation of the underwater turbulence and its effects on laser-based UOWC and imaging systems [6-14].

The use of the precise probability density function (PDF) of the received optical power is important in system modeling and bit error rate (BER) analysis [15]. However, not much experimental research has been reported on this within the context of UOWC systems. Lognormal distribution has been adopted in recent theoretical works with no experimental verifications [16-18]. In [19] the PDF of the received optical power for a UOWC link of 1 m long injected with bubbles was obtained [19]; however, the fluctuations in the optical power level due to bubbles was not considered as in the general case of underwater turbulence. In [20] heaters were used to create a temperature gradient of roughly 0.025° C per cm, which corresponds to weak turbulence with a scintillation index (SI) of less than 0.02 over a 1 m long water tank. In [21] for a temperature difference of up to 20° C between both ends of a channel (i.e., a 1 m long water tank) a SI of 0.1 was reported and it was shown that the PDF of received signal fitted well with Gamma and generalized Gamma distributions. However, in [21] the generated turbulence was not uniform throughout the water tank and therefore the propagating laser beam did not experience the same channel conditions. In [7], the influence of turbulence on the propagating laser beam was investigated in clear ocean water over a vertical path length of 8.75 m, where the index of refraction structure constant was extracted from the beam deflection; but with no results for the irradiance PDFs.

Due to the limitations of above mentioned experimental conditions including bubble injection, short length water tank and non-uniform turbulence, there is the need for detailed experimental tests and measurements in order to obtain the PDF of the received optical power. In this paper, we have developed an experimental test bed for UOWC where uniform turbulence is created by means of injecting water along the optical beam propagation path within a water pool over a transmission range of up to 12 m. A range of turbulence levels was

created by changing both the temperature T and the flow rate of the injected water Q in order to determine PDFs of the received optical power, the SI variations and the turbulence induced power loss for a range of link spans. Note that, in UOWC systems, the link span is one of the main factor influencing the received power fluctuations under turbulence conditions; however, to the best of our knowledge no research on the effects of turbulence over longer channel spans have been reported yet. Finally, we compare the measured results with generated data based on the model given in [22] and show that there is a good correlation between them.

2. MEASUREMENT SETUP

Fig. 1 shows the schematic block diagram and the experimental test-bed used in this work. At the transmitter (Tx), we used a fiber-pigtailed laser diode (LP520-SF15) at a typical wavelength of 520 nm, which was driven with a constant current source. A 3-axis microblock stage was used to align the laser output beam with the focal point of a bi-convex lens, which was used for beam collimation. Two identical periscopes were used at the Tx and the receiver (Rx) to launch the collimated optical beams into and out of the water pool. A bi-convex lens focused the light beam into an optical Rx composed of a Si photodetector and a transimpedance amplifier (PDA10A-EC). The field of view (FOV) of the Rx is calculated as [23]. The Rx's output voltage was converted into a digital format using Advantech USB-4716 data acquisition module at a sampling frequency of 5 kHz.

We used an indoor water pool with the dimensions of 3×1.77×100 m^3. The pool water temperature was between 22-23° C during the measurement campaign and its attenuation coefficient was measured to be 0.03 m^{-1} using a UV-2100 spectrophotometer at a wavelength of 520 nm, and multiple scattering was considered to be negligible. All the key system parameters adopted are listed in Table 1. The optical devices both at the Tx and the Rx sides were attached to configurable optical benches. While the Tx stage was fixed, the Rx was positioned on a moveable carriage platform located above the pool.

Table 1. System parameters

Parameter		Value
Underwater channel	Link span	3.5,5,7,10,12 m
	Water temperature	22-23° C
	Attenuation coefficient	0.03 m^{-1}
	Water depth	1.77 m
Periscopes	Pipe length	1.5 m
	Pipe diameter	12.5 cm
Laser diode	Wavelength	520 nm
	Maximum power	15 mW
Optical Rx	Output voltage	0-10 V
	PD active area	0.8 mm^2
	Wavelength range	200-1100 nm
	PD responsivity	0.44 A/W
	Gain	10^4 V/A
	Small signal bandwidth	150 MHz
Lens	Type	Bi-convex
	Diameter	50.8 mm
	Focal length of Tx & Rx	100, 150 mm
ADC	Sampling frequency	5 kHz

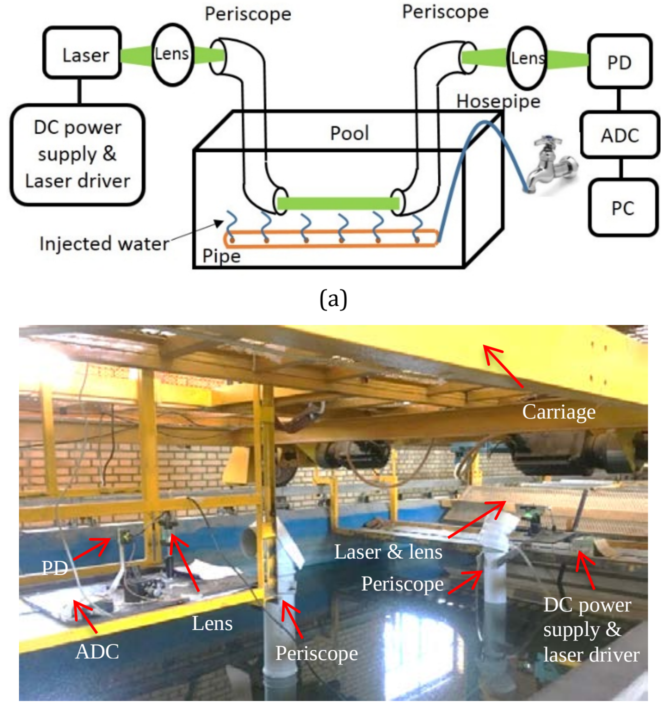

Fig. 1. The UOWC system: (a) the block diagram, and (b) the experimental test-bed

To create turbulence within the pool along the laser beam propagation path, we used a pipe with the length and diameter of 12 m and 3 cm, respectively, which was suspended 5 cm below the propagating laser beam, see the block diagram in Fig. 1(a) and the experimental test-bed in Fig. 2. To create a uniform turbulence, regular small holes of a 2 mm diameter at a spacing of 20 cm were made on the pipe facing upwards to inject water flow into the pool along the laser beam propagation path. One end of the pipe was attached to a hosepipe with a valve while the other end was blocked to ensure water being injected from the holes. We created a uniform turbulence along the laser beam propagation path by injecting cold and hot waters through the pipe at T of 22° C and 55° C, respectively and also by changing the Q (i.e., 200 mL/s, 180 mL/s and 90 mL/s).

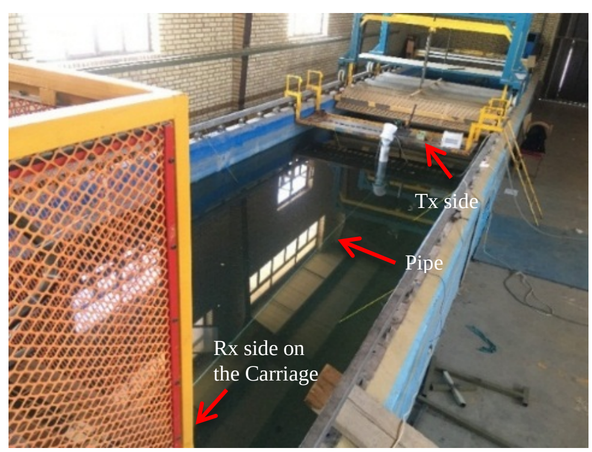

Fig. 2. Pipe installation exactly below the laser propagation path in a 12 m link span

3. RESULTS

We carried out measurements for link spans of 3.5, 5, 7, 10 and 12 m with and without turbulence. Fig. 3(a) shows the measured output signal voltage V_i normalized to its mean value for a 12 m link span, T = 55 °C and Q = 180 mL/s. It is clear from Fig. 3(a) that, in addition to high frequency fluctuations due to turbulence, there is also some low frequency fluctuations. The low frequency fluctuations, which is called beam wandering, was mostly due to uncontrolled mechanical vibration of both the Tx and Rx optical benches and the periscopes during data acquisition, which needs addressing.

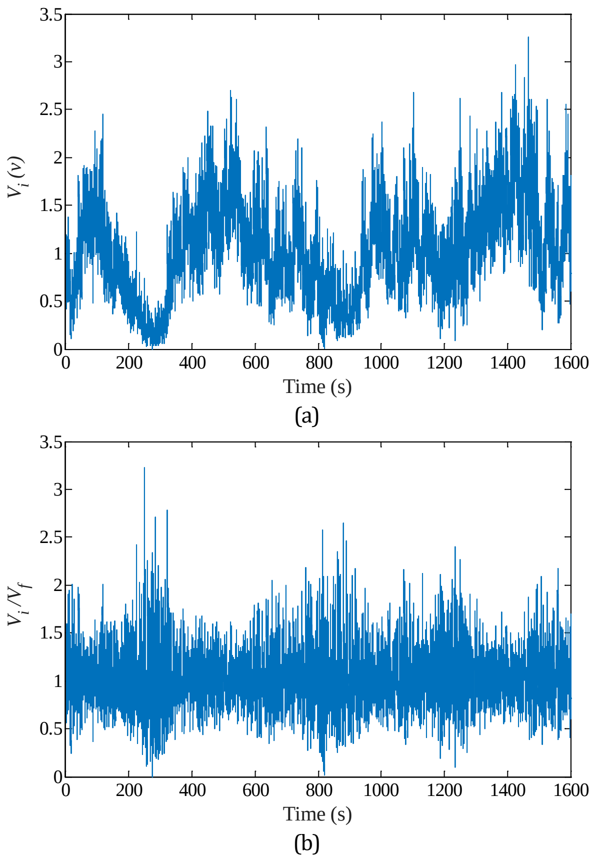

Fig. 3. For a 12 m link span, T = 55 °C and Q = 180 mL/s (a) V_i as a function of time, and (b) V_i/V_f as a function of time

To reduce beam wandering, V_i was normalized to its local average V_f, see Fig. 3(b) and Fig. 4 [7, 24]. The local average of V_i was obtained by passing V_i through a 3rd order Butterworth low-pass filter with a very low cut-off frequency of 0.04 Hz. Note that, the beam wandering induced fluctuations is below 0.04 Hz. Thus, after normalization the signal amplitude variation was considered in the SI calculation implicitly.

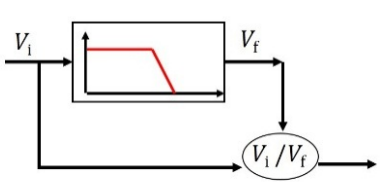

Fig. 4. V_i normalization

A. PDF of the received optical signal

In this section, PDFs of the ratio of the V_i/V_f for four different turbulence states - state 1 (no injected water), state 2 (T = 22 °C, Q = 90 mL/s), state 3 (T = 22 °C, Q = 200 mL/s) and state 4 (T = 55 °C, Q = 180 mL/s) - over a link span of 12 m are investigated. Fig. 5 compares the measured data with the lognormal distribution and the simulated results using the model in [22] for all states for a 12 m link span. Δz and R_i are the width of consecutive turbulent layers and the radius of curved boundaries as defined in [22]. All the key system model parameters are shown in Table 2.

Table 2. System model parameters

Parameter	Value
The refractive index variation range for each layer	[1.3365– $\Delta n/2$, 1.3365 + $\Delta n/2$]
Link span	3.5, 5, 7, 10, 12 m
Beam width	15 mm
Rx aperture diameter	50 mm
Δz	5 cm
R_i	0.01×|Ln (q)|
q	random number ∈ [0, 1]

In these plots we show the fitted well-known lognormal PDF distribution on the measured and simulated PDFs, which is given by [25]:

$$p(I) = \frac{1}{I\sigma_I\sqrt{2\pi}} \exp\left\{ -\frac{\left[\ln\left(\frac{I}{I_0}\right) + \frac{1}{2}\sigma_I^2 \right]^2}{2\sigma_I^2} \right\}, I > 0 \quad \textbf{(1)}$$

The results show that, the lognormal distribution match well with both the experiment and simulated data for up to SI of 0.07 for a 12 m link span for all states, thus confirming the accuracy of the proposed model. Similar results were observed for other link spans, which are not presented here.

The refractive index variation Δn is one of the important factor influencing the turbulence strength as in the model reported in [22]. By adapting the model of [22] to the four turbulence states, Δn values are 1e-6, 4.4e-6, 7e-6 and 308e-6 for the states of 1, 2, 3 and 4, respectively. Note that, for the state 4 turbulence is due to both high T and Q, thus the highest Δn variation was observed.

B. SI variation with the link span

Fig. 6 compares the measured and the simulated SI values as a function of the link span using the model in [22] for the states 1, 2 and 3. The SI values are obtained using the following equation:

$$\sigma_I^2 = \frac{\langle I^2 \rangle - \langle I \rangle^2}{\langle I \rangle^2} \quad \textbf{(2)}$$

where I is the V_i/V_f . As shown, SI increases with the link span for all states, and the measured values are very close to the predicted (modelled) data. For the state 1, we measured the natural turbulence of the pool water, which is more pronounced for the 10 and 12 m link spans.

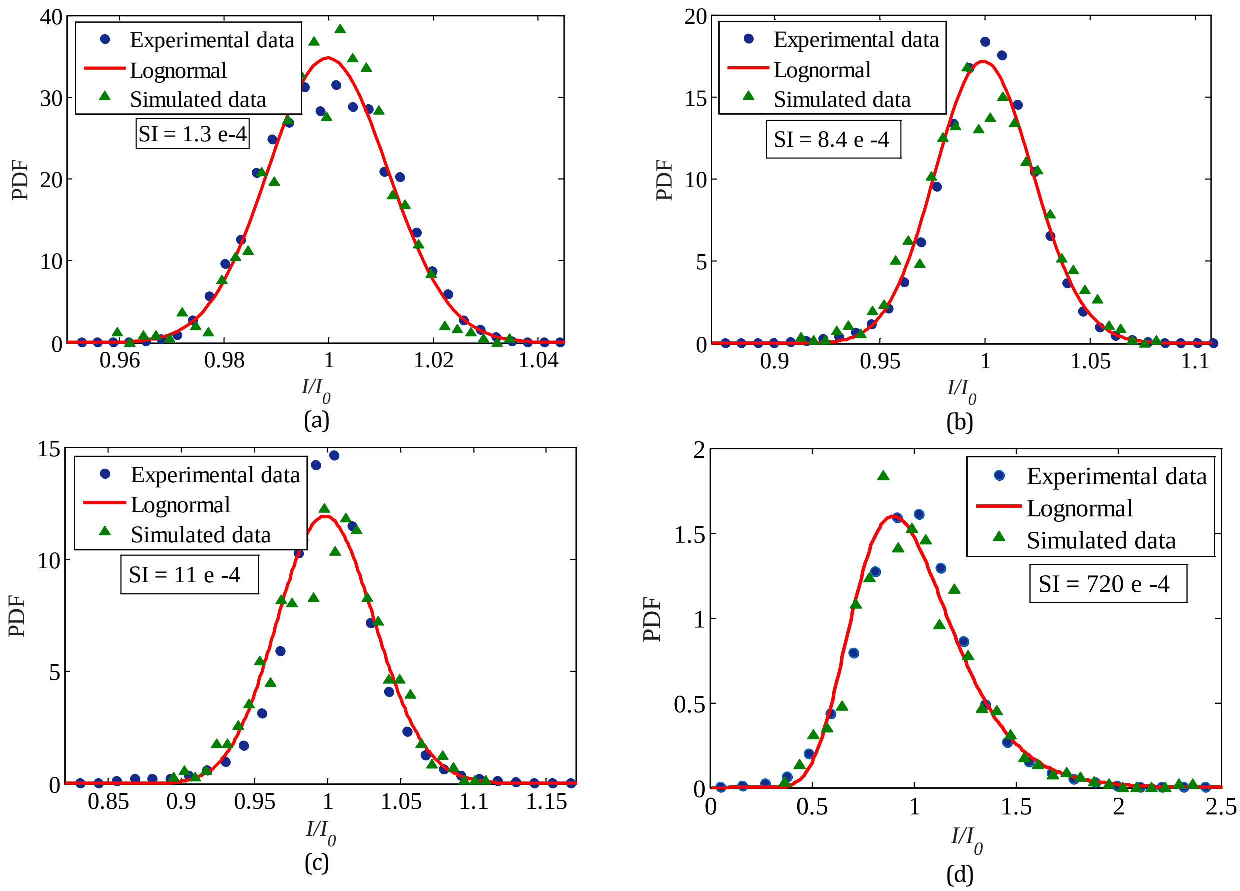

Fig. 5. PDFs of the experimental and simulated data fitted with lognormal distribution for a 12 m link span and for states: (a) 1, (b) 2, (c) 3, and (d) 4

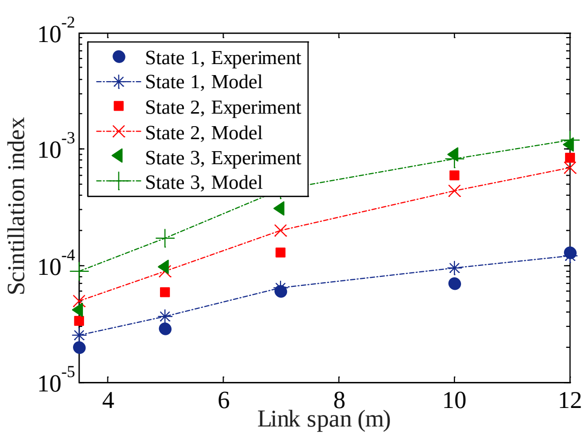

Fig. 6. Experiment and predicted SI values versus the link span for the State 1, 2 and 3

C. Turbulence induced power loss

The measured and predicted turbulence-induced power losses as a function of the states for a range of link spans (i.e., 3.5, 7 and 10 m) are depicted in Fig. 7. Note that, in here we determined the average value of the measured signal for different states for a specific link span and then normalized it to the average of the measured signal of the state 1 for the same link span and then compared the relative values. As shown in Fig. 7, higher power losses are observed for the state 4 with the highest measured and simulated SI values. Note that, for the state 4 the received optical beam area is larger than the Rx lens due to the simultaneous effects of beam spreading, beam wandering and scintillation, which results in the increased power loss compared to the other three states. This presents a noticeable power loss under high scintillation indices.

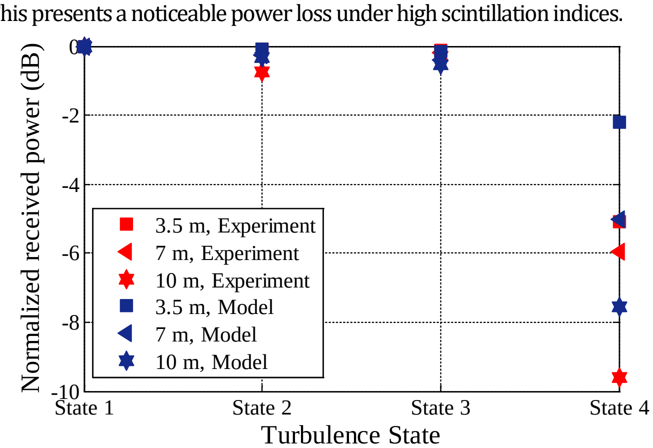

Fig. 7. Turbulence induced power loss in the experiment and model in 4 states

4. CONCLUSION

In this research the effect of turbulence on the UOWC system was investigated. A uniform turbulence was created by injecting water along

the optical beam propagation path within a pool to obtain the PDF of the received optical power. Different turbulence strengths were created by changing the temperature and the injected water flow rate. We showed that under different turbulence strengths there is a good fit between the PDFs of the experimental data with the lognormal distribution up to a scintillation index of around 0.07 over a 12 m link span. Variations of the scintillation index with the link span for a range of turbulence strengths were also presented. In addition, it was shown that the link experienced high power loss under turbulence. Finally, the experimental results were compared with our previously proposed turbulence model demonstrating a good match between them, thus confirming the accuracy of the proposed model.

Acknowledgment. The authors are grateful to Hossein Riahi, Raouf Sayed Tabatabaei, Mohammad Haji Jafari and Amir Mostashfi for their help during experimental investigation, and Hamed Noori for discussion on MATLAB based simulations.

References

1. G. Baiden, Y. Bissiri, and A. Masoti, "Paving the way for a future underwater omni-directional wireless optical communication systems," Ocean Eng. **36**(9-10), 633-640 (2009).
2. F. Hanson and S. Radic, "High bandwidth underwater optical communication," Appl. Opt. **47**(2), 277-283 (2008).
3. M. Uysal, C. Capsoni, Z. Ghassemlooy, A. Boucouvalas, and E. Udvary, *Optical Wireless Communications: An Emerging Technology* (Springer, 2016).
4. M. Kong, B. Sun, R. Sarwar, J. Shen, Y. Chen, F. Qu, J. Han, J. Chen, H. Qin, and J. Xu, "Underwater wireless optical communication using a lens-free solar panel receiver," Opt. Commun. **426,** 94-98 (2018).
5. M. Kong, Y. Chen, R. Sarwar, B. Sun, Z. Xu, J. Han, J. Chen, H. Qin, and J. Xu, "Underwater wireless optical communication using an arrayed transmitter/receiver and optical superimposition-based PAM-4 signal," Opt. Express **26**(3), 3087-3097 (2018).
6. G. Nootz, S. Matt, A. Kanaev, K. P. Judd, and W. Hou, "Experimental and numerical study of underwater beam propagation in a Rayleigh–Bénard turbulence tank," Appl. Opt. **56**(22), 6065-6072 (2017).
7. G. Nootz, E. Jarosz, F. R. Dalgleish, and W. Hou, "Quantification of optical turbulence in the ocean and its effects on beam propagation," Appl. Opt. **55**(31), 8813-8820 (2016).
8. Y. Ren, L. Li, Z. Zhao, G. Xie, Z. Wang, N. Ahmed, Y. Yan, A. Willner, Y. Cao, and C. Liu, "4 Gbit/s underwater transmission using OAM multiplexing and directly modulated green laser," in CLEO: Science and Innovations, (Optical Society of America, 2016), paper SW1F. 4.
9. Y. Ren, L. Li, Z. Wang, S. M. Kamali, E. Arbabi, A. Arbabi, Z. Zhao, G. Xie, Y. Cao, and N. Ahmed, "Orbital angular momentum-based space division multiplexing for high-capacity underwater optical communications," Scientific Reports **6,** 33306 (2016).
10. W. Hou, S. Woods, E. Jarosz, W. Goode, and A. Weidemann, "Optical turbulence on underwater image degradation in natural environments," Appl. Opt. **51**(14), 2678-2686 (2012).
11. W. Hou, S. Woods, W. Goode, E. Jarosz, and A. Weidemann, "Impacts of Optical Turbulence on Underwater Imaging," Proc. SPIE 8030, 803009 (2011).
12. A. V. Kanaev, W. Hou, S. Woods, and L. N. Smith, "Restoration of turbulence degraded underwater images," Opt. Eng. **51**(5), 057007 (2012).
13. B. Redding, A. Davis, C. Kirkendall, and A. Dandridge, "The influence of underwater turbulence on optical phase measurements," Proc. SPIE 9827, 982707 (2016).
14. S. Matt, W. Hou, W. Goode, and S. Hellman, "Introducing SiTTE: A controlled laboratory setting to study the impact of turbulent fluctuations on light propagation in the underwater environment," Opt. Express **25**(5), 5662-5683 (2017).
15. Z. Ghassemlooy, W. Popoola, and S. Rajbhandari, *Optical Wireless Communications: System and Channel Modelling with Matlab* (CRC Press, 2012).
16. S. A. Arpali, Y. Baykal, and Ç. Arpali, "BER evaluations for multimode beams in underwater turbulence," J. Mod. Opt. **63**(13), 1297-1300 (2016).
17. A. C. Boucouvalas, K. P. Peppas, K. Yiannopoulos, and Z. Ghassemlooy, "Underwater optical wireless communications with optical amplification and spatial diversity," IEEE Photon. Technol. Lett. **28**(22), 2613-2616 (2016).
18. M. V. Jamali, F. Akhoundi, and J. A. Salehi, "Performance characterization of relay-assisted wireless optical CDMA networks in turbulent underwater channel," IEEE Trans. Wireless Commun. **15**(6), 4104-4116 (2016).
19. M. V. Jamali, P. Khorramshahi, A. Tashakori, A. Chizari, S. Shahsavari, S. AbdollahRamezani, M. Fazelian, S. Bahrani, and J. A. Salehi, "Statistical distribution of intensity fluctuations for underwater wireless optical channels in the presence of air bubbles," in Iran Workshop on Communication and Information Theory (IWCIT) (IEEE, 2016), pp. 1-6.
20. M. P. Bernotas and C. Nelson, "Probability density function analysis for optical turbulence with applications to underwater communications systems," Proc. SPIE 9827, 98270D (2016).
21. H. M. Oubei, E. Zedini, R. T. ElAfandy, A. Kammoun, M. Abdallah, T. K. Ng, M. Hamdi, M. S. Alouini, and B. S. Ooi, "Simple statistical channel model for weak temperature-induced turbulence in underwater wireless optical communication systems," Opt. Lett. **42**(13), 2455-2458 (2017).
22. Z. Vali, A. Gholami, Z. Ghassemlooy, D. G. Michelson, M. Omoomi, and H. Noori, "Modeling turbulence in underwater wireless optical communications based on Monte Carlo simulation," J. Opt. Soc. Am. A **34**(7), 1187-1193 (2017).
23. C. Gabriel, M. A. Khalighi, S. Bourennane, P. Léon, and V. Rigaud, "Misalignment considerations in point-to-point underwater wireless optical links," in MTS/IEEE OCEANS-Bergen (IEEE, 2013), pp. 1-5.
24. M. Ouassou, O. Kristiansen, J. G. Gjevestad, K. S. Jacobsen, and Y. L. Andalsvik, "Estimation of scintillation indices: a novel approach based on local kernel regression methods," Int. J. Navi. Observ. **2016,** 1-18 (2016).
25. L. C. Andrews, R. L. Phillips, and C. Y. Hopen, *Laser Beam Scintillation with Applications* (SPIE Press, 2001).